論文 / 著書情報
Article / Book Information

Title	Growth mode and electronic structure of silver on ZnO(10-10)
Author	K. Ozawa, T. Sato, M. Kato, K. Edamoto
Journal/Book name	Surface Review and Letters, Vol. 13, No. 2 & 3, pp. 227-233
Issue date	2006, 4
URL	http://www.worldscientific.com/worldscinet/srl
DOI	http://dx.doi.org/10.1142/S0218625X06008116
Copyright	(c) copyright World Scientific Publishing Company.
Note	このファイルは著者（最終）版です。 This file is author (final) version.

GROWTH MODE AND ELECTRONIC STRUCTURE OF SILVER ON ZnO($10\bar{1}0$)

K. OZAWA*, T. SATO, M. KATO
Department of Chemistry and Materials Science, Tokyo Institute of Technology, Ookayama, Meguro-ku, Tokyo 152-0033, Japan

K. EDAMOTO
Department of Chemistry, Rikkyo University, Nishi-Ikebukuro, Toshima-ku, Tokyo 171-8501, Japan

The growth mode and electronic structure of the vapor-deposited Ag overlayer on the ZnO($10\bar{1}0$) surface is investigated by angle-resolved photoemission spectroscopy utilizing synchrotron radiation. The coverage dependent measurements of the two-dimensional band structure by the Ag 4*d* states reveal that the bands with a dispersing feature are developed from the low coverage region, suggesting that the Ag adatoms aggregate to from clusters with a laterally ordered structure. The Ag clusters grow in size with increasing the Ag coverage whereas the ordered atomic structure of the Ag cluster is preserved. From the analysis of the Ag 5*sp* band, the Ag clusters have a non-metallic electronic structure at low coverages, and the metallic nature is developed as the size of the clusters becomes enlarged.

Keywords: Silver; Zinc oxide; Cluster; Angle-resolved photoemission spectroscopy; Electronic structure.

1. Introduction

Metals deposited on metal oxide surfaces often exhibit properties that those in the bulk form do not possess. A well-known example is gold. Gold is the noblest of all metals so that chemical reactivity is quite low in the bulk form. However, Haruta et al. have found that gold clusters with the nanometer size supported on oxide surfaces exhibit a high catalytic activity.[1] Extensive studies have been carried out since then to elucidate the origin of the activity of gold nanoparticles, and the importance of the morphology and electronic structure of the gold nanoparticles is suggested.[2, 3, 4, 5] However, the complete understanding of how gold gains such a chemical activity in a particular condition is far from satisfactory.

Gold and other noble metals (Ag and Cu) tend to aggregate into clusters on metal oxide surfaces. This is because (1) the oxide surfaces, in general, have lower surface free energies than those of noble metals and (2) only a weak noble-metal/oxide interface interaction is emerged, largely owing to the low heat of oxide formation of noble metals.[6] Noble metals on the ZnO surfaces are not exception: Recent scanning tunneling microscopy (STM) studies have shown that Cu atoms aggregate into two-dimensional and three-dimensional clusters on the (0001)-Zn, ($000\bar{1}$)-O and ($10\bar{1}0$) surfaces of single crystal ZnO.[7, 8] Photoelectron spectroscopy (PES) studies have also suggested the cluster formation of Au on the ZnO(0001)-Zn and ZnO($000\bar{1}$)-O surfaces[9] and of Ag on the polycrystalline ZnO surface.[10] These noble-metal/ZnO systems are found to be good catalysts for methanol synthesis.[11, 12, 13] Therefore, it is desired to investigate the morphology and the electronic structure of the metal clusters on the ZnO surfaces in order to understand the catalytic reactivity

*Corresponding author. E-mail: kozawa@chem.titech.ac.jp

of the noble-metal/ZnO systems.

In this paper, we present the result of the study on the growth mode and the electronic structure of the Ag overlayer on the ZnO($10\bar{1}0$) surface using angle-resolved photoemission spectroscopy (ARPES). It is found that the Ag adatoms form clusters with a laterally ordered atomic structure and these clusters grow in size with increasing the Ag coverage. The small Ag clusters have a nonmetallic electronic structure, whereas the metallic nature is brought about in the larger clusters.

2. Experimental

The ARPES measurements were carried out at the beam line 11C of the Photon Factory, High Energy Accelerator Research Organization (KEK), where synchrotron light was dispersed by a Seya-Namioka monochromator. Photoelectrons were collected by an electron energy analyzer with an acceptance angle of $\pm$ 1°. The total energy resolution, estimated from the Fermi edge of the spectra from the Ta holder, was 0.2 eV at photon energy $h\nu$ of 20 eV. The ultrahigh vacuum (UHV) chamber was also equipped with a single pass cylindrical mirror analyzer (CMA) for the Auger electron spectroscopy (AES) measurements, low energy electron diffraction (LEED) optics and a quadrupole mass spectrometer. The base pressure of the UHV system was 2×10^{-10} Torr. All the measurements were carried out at RT.

The ZnO single crystal with the ($10\bar{1}0$) orientation ($10 \times 7 \times 0.5$ mm^3; Yamanaka Semiconductor Co.) was mounted on the Ta holder. The sample surface was cleaned by cycles of Ar^+ sputtering (1.6 kV, 2–3 μA) and annealing at 1050 K in UHV, and annealing at 700 K in O_2 atmosphere and 600 K in UHV were carried out in order to compensate the O defects at the surface. More detailed procedure is found elsewhere.[14] The cleanliness of the surface was checked by the AES spectra, which showed no peaks associated with contaminants such as carbon, and the surface thus prepared showed sharp (1×1) LEED spots.

Ag was vapor-deposited onto the surface at room temperature using a commercial evaporation source. The pressure during the deposition was kept below 8×10^{-10} Torr so that contaminant-free Ag deposited surfaces were prepared as proved by the AES measurements.

3. Results and discussion

As the ZnO($10\bar{1}0$) surface is being covered with Ag, the Ag MNN Auger peak grows at 350 eV, while the intensities of the O KLL (510 eV) and Zn LMM (985 eV) peaks are slightly diminished in the AES spectra. In Fig. 1, we plotted the Auger peak-to-peak intensity ratios of Ag MNN/O KLL and Ag MNN/Zn LMM against Ag deposition time. Both intensity ratios increase linearly with increasing the deposition time. However, the increasing rate diminishes at times longer than 5.5 min, forming a kink point in each line. We temporarily assigned this point to be 1 monolayer (ML), and the Ag coverage Θ_{Ag} is given by the Ag MNN/O KLL ratio relative to that at 1 ML.

In the inset of Fig. 1, a typical example of the Auger spectra for the 1-ML Ag-covered ZnO($10\bar{1}0$) surface is shown as curve (a). Curve (b) is the Auger spectrum for the c(10×2)Ag/Cu(001) surface, which we measured with the same experimental condition as that employed in the study for the Ag/ZnO($10\bar{1}0$) system. Thus, the parallel comparison of the peak intensity is possible between these two spectra. From an inspection of the AES spectra shown in the inset, the Ag MNN peak-to-peak intensities for the two Ag adsorption systems are the same within the experimental error ($\sim 5\%$). This implies that the Ag adatom density at 1 ML on ZnO($10\bar{1}0$) can be roughly estimated to be the same as that for the c(10×2)Ag/Cu(001) surface, i.e., 1.38×10^{15} cm^{-2}.[15, 16]

Fig. 2(a) shows normal emission spectra of ZnO($10\bar{1}0$) covered with different amount of Ag. The spectrum of the clean surface bears an asymmetric triangular peak at 3–7 eV, which is formed by emissions from the O 2p dangling bond state and the O 2p–Zn 3d/4sp hybrid states. A slight hump at 8 eV is also attributed to the O–Zn hybrid state, and a sharp peak at 10–12 eV arises from the Zn 3d states. Details on the valence

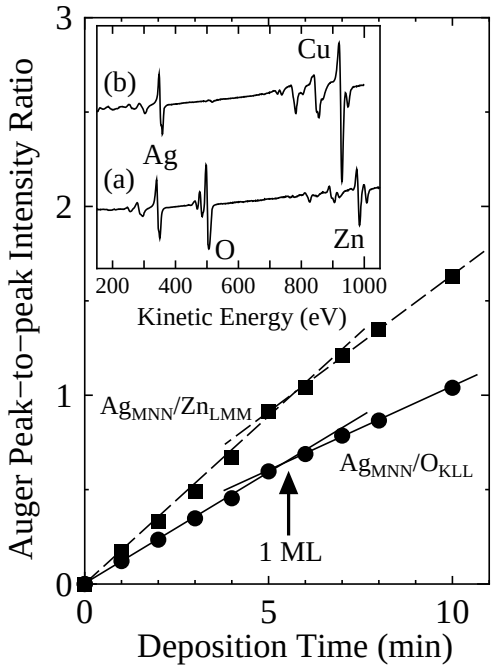

Fig. 1. Auger peak-to-peak intensity ratio of Ag MNN/O KLL (filled circles) and Ag MNN/Zn LMM (filled squares) as a function of the Ag deposition time for the Ag/ZnO(10$\bar{1}$0) system. A break point at 5.5-min deposition is defined as 1 ML of the Ag coverage. The inset shows the Auger spectra for (a) the 1-ML Ag-covered ZnO(10$\bar{1}$0) surface and (b) the c(10×2)Ag/Cu(001) surface. The primary energy of the electron beam was 2 keV.

electronic structure of the clean surface are given in Ref. 17. These substrate-originated emission peaks are attenuated by Ag adsorption, whereas the Ag 4*d* peaks grow at 4–8 eV. We have identified, by taking second derivatives of the raw spectra, five Ag 4*d* peaks (4.3, 4.9, 5.7, 6.2 and 7.2 eV) as marked by bars. These Ag 4*d* states form two-dimensional bands within the Ag overlayer at $\Theta_{\rm Ag} = 1.3$ ML. This is because they exhibit an energy dispersion as a function of the surface parallel component of the wave vector ($k_{\parallel}$) as shown in Fig. 3, whereas the binding energy of each Ag 4*d* state is independent on the surface perpendicular component of the wave vector ($k_{\perp}$).[18] The lack of the energy dispersion in $k_{\perp}$ implies that the deposited Ag overlayer is at most a few atomic-layer thickness at 1.3 ML.

Fig. 2(b) shows the enlarged spectra around the Fermi level ($E_{\rm F}$) for the Ag/ZnO(10$\bar{1}$0) surface. A step-like emission structure by the Ag 5*sp* band is developed in the band gap region of ZnO. An interesting feature of this emission structure is the $\Theta_{\rm Ag}$ dependence of the onset position; it locates at 0.7 eV below $E_{\rm F}$ at 0.1 ML and shifts monotonically to reach $E_{\rm F}$ at 1.05 and 1.3 ML. We plot the onset position as a function $\Theta_{\rm Ag}$ in the inset of Fig. 2(b). The off-normal emission spectra also show a similar $\Theta_{\rm Ag}$-dependent change of the step structure by the Ag 5*sp* band. Thus, the step structure shown in Fig. 2(b) should represent the total density of states (DOS) of the Ag 5*sp* states. The shift of the onset of the step-like *sp* DOS is commonly observed for the noble-metal adsorption systems, where adatoms aggregate to form clusters and these clusters grow in size with increasing coverages.[19, 20, 21] Therefore, the shift of the onset energy of the Ag 5*sp* DOS is indicative of the cluster formation of deposited Ag on ZnO(10$\bar{1}$0) at room temperature.

The $\Theta_{\rm Ag}$-dependent measurements of the Ag 4*d* band structure also support the cluster formation of Ag. Fig. 3 shows gray-scale two-dimensional band maps along the $\overline{\Gamma X'}$ axis of the surface Brillouin zone of

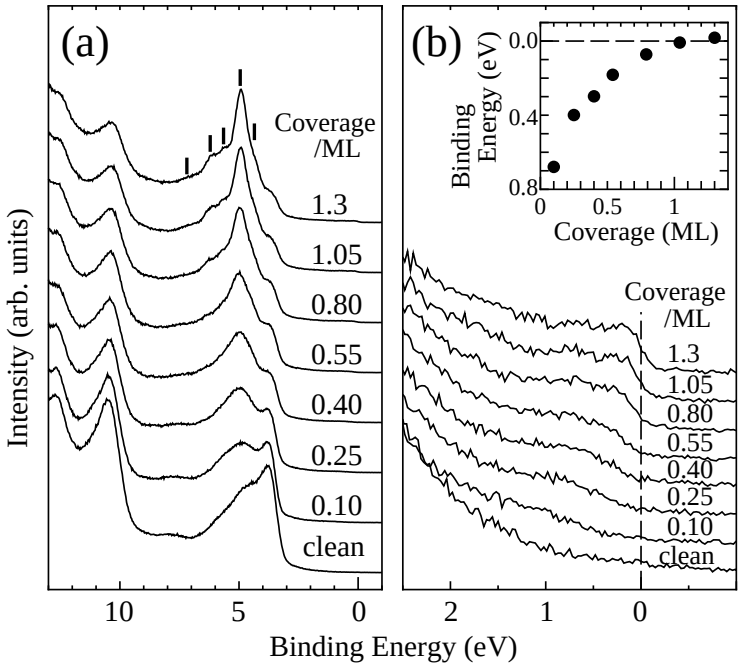

Fig. 2. (a) Normal emission spectra of ZnO($10\bar{1}0$) as a function of Θ_{Ag}. The spectra were taken with the photon energy of 20 eV and the incident angle of the light of 50° measured from the surface normal direction. The positions of the five Ag 4*d* peaks are indicated by tick marks. (b) The enlarged spectra around E_{F}. The binding energy of the onset position of the step structure is plotted as a function of Θ_{Ag} in the inset.

ZnO($10\bar{1}0$) for the Ag-covered surfaces with three different coverages. On the ZnO($10\bar{1}0$) surface covered with a sufficient amount of Ag ($\Theta_{\mathrm{Ag}} = 1.3$ ML), several Ag 4*d* bands are observed in the energy region between 4 and 8 eV (labeled A–G). Some of these bands show strong dispersion, indicating a sufficient orbital interaction between the neighboring Ag adatoms. The emission intensity from the Ag 4*d* bands becomes weaker as Θ_{Ag} decreases from 1.3 to 0.12 ML, and only a faint emission is observed at 0.12 ML. However, we still see the Ag 4*d* states forming dispersing bands. This means that the lateral Ag–Ag interaction is sufficiently strong even at 0.12 ML. In order to establish such an interaction between the Ag adatoms at 0.12 ML, each Ag atom should be condensed into clusters. Thus, the Θ_{Ag} dependence of the two-dimensional Ag 4*d* band structure suggests the Ag cluster formation.

Since the two-dimensional electronic structure is realized in the Ag overlayer despite the formation of the Ag clusters as discussed above, the band structure of the Ag 4*d* states should reflect the laterally ordered adatom structure. Fig. 3 shows that the periodicity of the Ag 4*d* band dispersion along the $\overline{\Gamma X'}$ axis (the [0001] direction) is different from that of the O 2*p* band, which is observed as a bright emission band at 3.5–4 eV at 0.12 ML. This implies that the periodic arrangement of the O atoms in the substrate surface and the Ag adatoms is different in the [0001] direction. One notices that the most intense branch (B) and the deepest-lying band (E), both of which exhibit strong dispersion among the Ag 4d bands, have symmetric dispersion around the $\overline{\Gamma_{\mathrm{2nd}}}$ point (the center of the second surface Brillouin zone) along $\overline{\Gamma X'}$ at 0.65 and 1.3 ML. This may suggest that $\overline{\Gamma_{\mathrm{2nd}}}$ point could be a boundary of the Brillouin zone for the Ag overlayer, i.e., the size of the Brillouin zone for the Ag overlayer is twice as that of the surface Brillouin zone for the ZnO($10\bar{1}0$) surface along the [0001] direction. A very simple model to explain the difference in size of the Brillouin zones is that the neighboring Ag–Ag distance is half of the O–O (or Zn–Zn) distance in the [0001] direction at high Θ_{Ag}

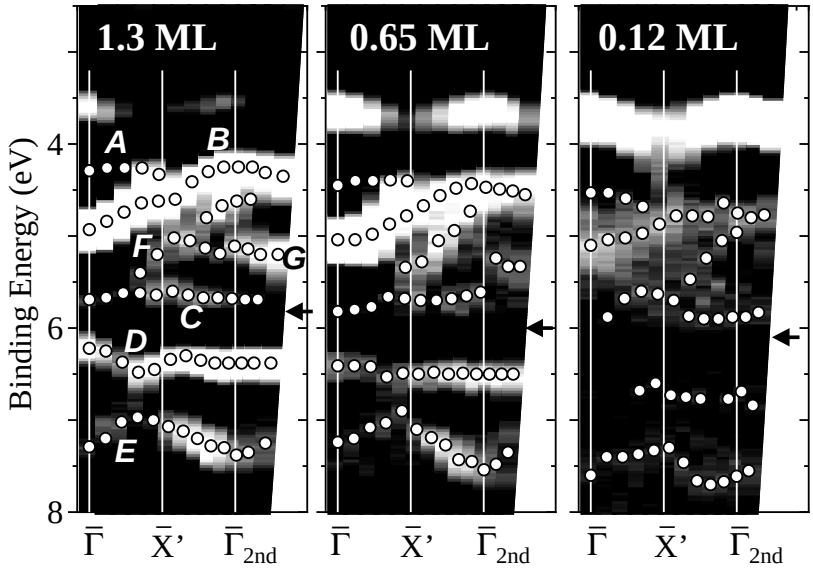

Fig. 3. The Θ_{Ag}-dependent change in the two-dimensional band structure of the Ag 4*d* states along the $\bar{\Gamma}\bar{X}'$ axis of the surface Brillouin zone of the substrate surface. Seven Ag 4*d* bands (A–G) are identified and are indicated by open circles. The arrows show the energetic center of the Ag 4*d* bands.

($\geq$ 0.65 ML), i.e. 0.26 nm. More detailed discussion on the local atomic structure of the Ag cluster is found in our recent paper.[18]

Summarizing the adsorption process of Ag on ZnO(10$\bar{1}$0), deposited Ag aggregates to form clusters from the low coverages, and these clusters grow in size with increasing Θ_{Ag}. However, each Ag clusters should be at most a few atomic-layer thickness up to 1.3 ML. From the dispersive feature of the Ag 4*d* bands, the laterally ordered atomic structure is considered to be formed within the Ag clusters.

A careful examination of the Θ_{Ag}-dependent change in the Ag 4*d* bands (Fig. 3) reveals that all Ag 4*d* bands shift to the lower binding energy side with increasing Θ_{Ag}. The energetic center of the 4*d* bands, indicated by arrows in Fig. 3, moves from 6.1 eV at 0.12 ML to 5.8 eV at 1.3 ML. As mentioned above, the energy shift towards E_F is also observed for the onset position of the Ag 5*sp* DOS, but with much larger magnitude (0.7 eV from 0.1 to 1.3 ML). Moreover, the peaks from the substrate surface shift to the lower binding energy side; the Zn 3*d* and O 2*p* peaks locate at 10.49 and 3.77 eV on the Ag-free surface, respectively, and move to 10.30 and 2.57 eV up to 1.3 ML [Fig. 2(a)]. Therefore, all peaks observed in the valence band spectra move to the lower binding energy side with increasing Θ_{Ag}. In Fig. 4, we summarize the Θ_{Ag}-dependent shift of the energetic center of the Ag 4*d* bands (open squares), the onset of the Ag 5*sp* DOS (filled circles), the Zn 3*d* peak (filled triangles) and the O 2*p* peak (open triangles). Here, the shifts are measured from the energetic positions at 1.3 ML.

It is often observed that metal adsorption on semiconductor surfaces induces bending of the substrate's bands at the surface. For the noble-metal/ZnO systems, downward band bending is observed for Cu/ZnO(000$\bar{1}$)-O,[22] while Cu on ZnO(0001)-Zn tends to induce upward bending.[23] Au deposition, on the other hand, leads to upward bending on three types of the ZnO surfaces, i.e., the polar (000$\bar{1}$)-O and (0001)-Zn surfaces [9] and the nonpolar (10$\bar{1}$0) surface.[24] Regarding the present Ag/ZnO(10$\bar{1}$0) system, since a similar coverage dependent shift is observed for both Zn 3*d* and O 2*p* peaks as shown in Fig. 4, bending of the ZnO bands should account for the observed peak shift. The shift towards the lower binding energy side means that the ZnO bands bend upward by Ag adsorption. The Fermi-level pinning does not take place up to Θ_{Ag} = 1.3 ML,

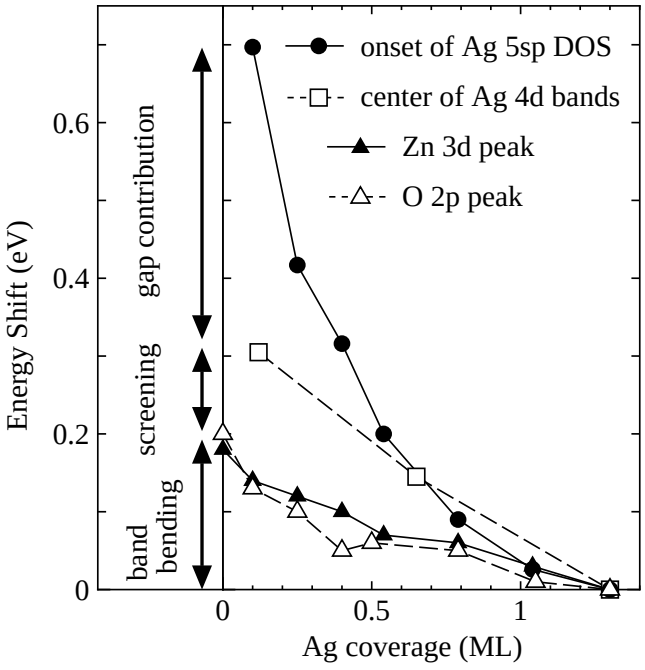

Fig. 4. The Θ_{Ag}-dependent shift of the O 2*p* and Zn 3*d* peak positions, the energetic center of the Ag 4*d* bands and the onset position of the Ag 5*sp* DOS. The magnitude of the shift is shown relative to the positions at $\Theta_{Ag} = 1.3$ ML.

because the continuous shift of the Zn 3*d* and O 2*p* peaks is observed up to this coverage. The magnitude of band bending is approximately 0.2 eV at 1.3 ML relative to the clean surface.

The shift of the energetic center of the Ag 4*d* bands is larger than Ag-induced band bending. We consider that the extra shift, which is ~ 0.15 eV at 0.1–0.2 ML and 0.1 eV at 0.6–0.7 ML, is owing to the final state effect of the Coulomb interaction between the emitted photoelectron and the photohole left in a cluster. A similar energy shift of the metal bands has also been found for the Ag and Pd clusters by Wertheim et al.,[19] and by Hövel et al.[20] According to the model by Hövel et al.,[20] the Coulomb potential felt by the photoelectron varies depending on the cluster size because of the different efficiency of hole screening by the valence electrons of the cluster, i.e., the smaller the cluster size is, the stronger Coulomb interaction operates because of lesser available valence charge to screen the photohole. This results in the energy shift of the metal bands to the higher binding energy side for the small clusters in comparison with bulk metal. For example, the shift of 0.6 eV from the bulk value is found for the Ag 4*d* band of the Ag clusters with ~ 20 atoms on amorphous carbon.[19] The cluster-size dependent shift of the metal *d* bands is also observed for $Au/TiO_2(110)$[21] and $Ag/TiO_2(110)$.[25] For the present $Ag/ZnO(10\bar{1}0)$ system, the adsorbed Ag atoms aggregate to from clusters from the low Θ_{Ag}, and these clusters grow with increasing Θ_{Ag}. Therefore, the total shift of the Ag 4*d* bands from 6.1 to 5.8 eV at 0.12 to 1.3 ML results from, in addition to the Ag-induced upward bending, the cluster size-dependent change of the final-state effect.

The final-state effect should affect the Ag 5*sp* and 4*d* states equally. Moreover, the contribution of the Ag-induced band bending of the substrate surface is also equivalent for both Ag 5*sp* and 4*d* states. Thus, the Θ_{Ag}-dependent shift of the onset energy of the Ag 5*sp* DOS should be equal to that of the energetic center of the Ag 4*d* bands unless other effects are operative. However, the deviation of the magnitude of the shift is apparent at $\Theta_{Ag} < \sim 0.6$ ML (Fig. 4). As discussed below, this should reflect the semiconducting nature of

the small Ag clusters.

The scanning tunneling spectroscopy (STS) study for the electronic structure of the Ag clusters on TiO_2(110)[26] has revealed that the small clusters have a semiconducting nature and the gap between the highest occupied molecular orbital (HOMO) state and the lowest unoccupied molecular orbital (LUMO) state opens around E_F. Growth of the Ag clusters results in the narrowing of the HOMO–LUMO gap and finally brings the metallic electronic structure at the cluster size of ~ 4 nm.[26] A similar gap closing with increasing the cluster size is observed for the Au clusters on TiO_2(110).[26] A nonmetallic nature of the small Ag clusters on ZnO(10$\bar{1}$0) is also expected so that the HOMO of the Ag cluster should locate below E_F as a result of gap opening, and the HOMO moves towards E_F with increasing the cluster size. The onset position of the Ag 5*sp* DOS corresponds to the HOMO level. Thus, the shift of the onset position must be affected by the cluster-size dependent nonmetal-to-metal transition. The extra shift of the onset of the Ag 5*sp* DOS in comparison with the Ag 4*d* bands is due to the gap opening in the small Ag clusters.

It is worth mentioning that, although the onset of the Ag 5*sp* DOS coincides with E_F at $\Theta_{Ag} \geq 1$ ML (Figure 2), the metallic band should already be formed at much lower coverages. Comparison of the Θ_{Ag}-dependent shift of the Ag 5*sp* DOS with that of the Ag 4*d* bands suggests that the HOMO–LUMO gap may close at ~ 0.6 ML. The appearance of the Fermi edge below F_F is due to the Coulomb interaction between the emitted photoelectron and the charged Ag cluster,[19, 20] i.e., the metallic screening is not yet realized in the Ag clusters in the coverage region between 0.6 and 1 ML.

4. Summary

The ARPES measurements have been carried out to elucidate the growth mode and the electronic structure of Ag deposited on the ZnO(10$\bar{1}$0) surface at room temperature. The Ag coverage dependence of the Ag 4*d* band structure shows that the Ag 4*d* bands with a dispersing feature are already formed at $\Theta_{Ag} = 0.12$ ML. A direct Ag–Ag interaction should be emerged in order to form the dispersing bands. Thus, the Ag adatoms are condensed to establish the Ag–Ag interaction, i.e., the Ag clusters are formed. Moreover, the formation of the dispersing bands means that each clusters have an atomically ordered structure. Increasing the Ag coverage results in the growth of the Ag clusters, but the local atomic structure is preserved because the Ag 4*d* band structure undergoes only a minor change. From the difference in the coverage-dependent shift of the energetic center of the Ag 4*d* bands and the onset of the Ag 5*sp* DOS, the Ag clusters should exhibit a nonmetallic nature at low coverages, whereas those at high coverages gain a metallic electronic structure.

Acknowledgments

A financial support from the Ministry of Education, Culture, Sports, Science and Technology of Japan (a Grants-in-Aid for Scientific Research) is greatly appreciated. This work was performed under the approval of the Photon Factory Advisory Committee (Proposal No. 2004G-007). We thank the staff of the Photon Factory for their excellent support.

References

1. M. Haruta, S. Tsubota, T. Kobayashi, H. Kageyama, M. J. Genet and B. Delmon, *J. Catal.* **144**, 175 (1993).
2. M. Valden, X. Lai and D. W. Goodman, *Science*, **281**, 1647 (1998).
3. M. S. Chen and D. W. Goodman, *Science*, **306**, 252 (2004).
4. B. Yoon, H. Häkkinen, U. Landman, A. S. Wörz, J.-M. Antonietti, S. Abbet, K. Judai and U. Heiz, *Science*, **307**, 403 (2005).
5. Z.-P. Liu, S. J. Jenkins and D. A. King, *Phys. Rev. Lett.* **94**, 196102 (2005).
6. C. T. Campbell, *Surf. Sci. Rep.* **27**, 1 (1997).
7. O. Dulub, L. A. Boatner and U. Diebold, *Surf. Sci.* **504**, 271 (2002).
8. L. V. Koplitz, O. Dulub and U. Diebold, *J. Phys. Chem.* **B107**, 10583 (2003).

9. B. J. Coppa, C. C. Fulton, S. M. Kiesel, R. F. Davis, C. Pandarinath, J. E. Burnette, R. J. Nemanich and D. J. Smith, *J. Appl. Phys.* **97**, 103517 (2005).
10. S. Chaturvedi, J. Rodriguez, T. Jirsak and J. Hrbek, *Surf. Sci.* **412/413**, 273 (1998).
11. M. S. Spencer, *Topics Catal.* **8**, 259 (1999).
12. H. Sakurai and M. Haruta, *Catal. Today*, **29**, 361 (1996).
13. S. Sugawa, K. Sayama, K. Okabe and H. Arakawa, *Energy Conserv. Mgmt.* **36**, 665 (1995).
14. K. Ozawa and K. Edamoto, *Surf. Sci.* **524**, 78 (2003).
15. J. G. Tobin, S. W. Robey and D. A. Shirley, *Phys. Rev.* **B33**, 2270 (1986).
16. P. T. Sprunger, E. Lægsgaard and F. Besenbacher, *Phys. Rev.* **B54**, 1863 (1996).
17. K. Ozawa, K. Sawada, Y. Shirotori, K. Edamoto, *J. Phys.: Condens. Matter*, **17**, 1271 (2005).
18. K. Ozawa, T. Sato, M. Kato, K. Edamoto, Y. Aiura, *J. Phys. Chem.* **B109**, 14619 (2005).
19. G. K. Wertheim, S. B. DiCenzo and D. N. E. Buchanan, *Phys. Rev.* **B33**, 5384 (1986).
20. H. Hövel, B. Grimm, M. Pollmann and B. Reihl, *Phys. Rev. Lett.* **81**, 4608 (1998).
21. A. Howard, D. N. S. Clark, C. E. J. Mitchell, R. G. Egdell and V. R. Dhanak, *Surf. Sci.* **518**, 210 (2002).
22. K. H. Ernst, A. Ludviksson, R. Zhang, J. Yoshihara and C. T. Campbell, *Phys. Rev.* **B47**, 13782 (1993).
23. J. Yoshihara, J. M. Campbell and C. T. Campbell, *Surf. Sci.* **406**, 235 (1998).
24. W. Göpel, L. J. Brillson and C. F. Brucker, *J. Vac. Sci. Technol.* **17**, 894 (1980).
25. K. Luo, T. P. St. Clair, X. Lai and D. W. Goodman, *J. Phys. Chem.* **B104**, 3050 (2000).
26. C. C. Chusuei, X. Lai, K. Luo and D. W. Goodman, *Topics Catal.* **14**, 71 (2001).